ABSTRACT

SMART POLYMERIC TEMPERATURE SENSORS – FOR BIOLOGICAL SYSTEMS

By
Greenee Anilkumar Sinha

The damaged brain is vulnerable to increase in brain temperature after a severe head injury. Continuous monitoring of intracranial temperature depicts functionality essential to the treatment of brain injury Many innovations have been made in the biomedical industry relying on electronic implants in treating condition such as traumatic brain injury (TBI) or other cerebral diseases. Hence, a methodical and reliable way to measure the temperature is crucial to assess the patient's situation. In this investigation, an analysis of various approaches to detect the change in the temperature due to resistance, current-voltage characteristics with respect to time has been evaluated. Also, studies describing various materials used in sensors, their working principles and the results anticipated in these discrete procedures are presented. These smart temperature sensors have provided the accuracy and the stability compared to earlier methods used to detect the change in brain temperature since temperature is one of the most important variables in brain monitoring.

SMART POLYMERIC TEMPERATURE SENSORS – FOR BIOLOGICAL SYSTEMS

by
Greenee Anilkumar Sinha

A Thesis
Submitted to the Faculty of
New Jersey Institute of Technology
in Partial Fulfillment of the Requirements for the Degree of
Master of Science in Materials Science and Engineering

Interdisciplinary Program in Materials Science and Engineering

May 2017

APPROVAL PAGE

SMART POLYMERIC TEMPERATURE SENSORS – FOR BIOLOGICAL SYSTEMS

Greenee Anilkumar Sinha

Dr.N.M. Ravindra, Thesis Advisor Date
Professor of Material Sciences and Engineering, NJIT

Dr. Sagnik Basuray, Committee Member, Date
Assistant Professor of Chemical, Biological and Pharmaceutical Engineering, NJIT

Dr. Michael Jaffe, Committee Member, Date
Research Professor of Biomedical Engineering, NJIT

Dr. Alex Stein, Committee Member, Date
Chief Executive Officer, Harmon Sensors Inc.

BIOGRAPHICAL SKETCH

Author: Greenee Anilkumar Sinha

Degree: Masters of Science

Date: May 2017

Undergraduate and Graduate Education:

- Master of Science in Materials Science and Engineering,
  New Jersey Institute of Technology, Newark, New Jersey, USA, 2017

- Bachelor of Science in Physics,
  Mithibai College, Mumbai University, Mumbai, India, 2014

Major: Materials Science and Engineering

ACKNOWLEDGMENT

Without the commitment of Dr. N.M. Ravindra this thesis could not have been completed. I would like to dedicate this Thesis to him, without his support and endurance, it would have been next to impossible to address this subject. In addition, I would also like to acknowledge everyone who helped me to get through my career especially my parents. I thank God for making me believe that I could accomplish this in my life.

I would also like to thank Professor Michael Jaffe, Professor Sagnik Basuray and Dr.Alex Stein who took some time out from their busy schedules and agreed to be a part of my thesis committee and review my thesis.

I would also like to thank my partner and my friends who always kept my moral high, supported me through all the tough nights and helped me to reduce my tension.

TABLE OF CONTENTS

LIST OF FIGURES

FIGURE **PAGE**

LIST OF FIGURES
(Continued)

CHAPTER 1

INTRODUCTION

Many great activities are linked to the brain and temperature. While brain temperature is largely dependent on the metabolic activity of brain tissue, the regulation of these two parameters is complex. Observational data has shown that the core body temperature and brain temperature can differ significantly. During injuries and infections in the patients, the temperature gradient between brain and the core is nearly ranging from +0.3 to +2℃. Prior to patient's death it was noticed that the body core temperature had exceeded the brain temperature. As an injured brain is extremely receptive and vulnerable to minuscule temperature variation. Therefore, an accurate and stable method to monitor the temperature change in brain is developed. Measuring the core body temperature only is not sufficient to monitor the cerebral status of TBI patients. External ventricular drain (EVD) are used in the treatments of patients with TBI or a hemorrhage.

The current approaches are susceptible from low temporal and spatial resolution, EVD related bacterial infections. Using the new approach of micro-electro-mechanical systems (MEMS) based fabrication technology allows association of multiple micro-sensors on both inside and outside of the flexible polymer tube while dodging wiring and assembling problems associated with previous methods. Recent growth in MEMS and nanotechnology permits the development of highly functional probes for diagnosis and treatment of brain diseases and injuries. The selection of MEMS technology has the probability to revolutionize brain multimodality monitoring by integrating all the desired function into a single unit.

To obtain accurate and real-time readings of the temperature variation, distinct implantable temperature sensors and probes have been developed using the principles of optical fiber, resistance temperature detector, thermocouple and thermistor. Starting with optical fiber, it is difficult to integrate the fibers into a single unit, for thermal mapping we require many fibers which will in turn increase the damage caused by fiber insertion. Major problem arises is because the detection system is sometimes complex and expensive. It requires a precise installation procedure and development of usable measuring system is complex.

The resistance temperature detector also known as resistance thermometers are used to measure the temperature consisting of a fine wire wrapped around a ceramic. Most of the times the RTD has an accurate resistance-temperature relationship provides an indication of temperature. To measure the resistance across an RTD, apply a constant current, measure the resulting voltage, and determine the RTD resistance. RTDs exhibit linear resistance to temperature curves over their operating regions, and any nonlinearity are highly predictable and repeatable. But even the RTD's have some of its limitations to work, first it's rarely used at temperatures above 600℃ as well as below -270℃ since the resistance then is mainly calculated by the impurities which independent of temperature. Thus, the sensitivity is essentially zero. These smart catheter temperature sensors are based with 4-probe wire configuration. It investigates 1) design, optimization and characterization of SCT's 2) development of mixed signal front end interface circuits for signal processing 3) development of portable monitor to record and analyze data 4) comparison of SCT's with commercial temperature probe based on accuracy and long term stability.

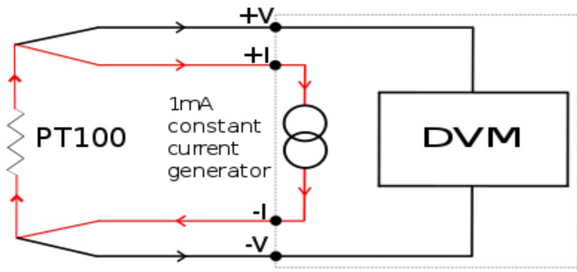

Figure 1.1 4-wire configuration of a RTD.
Source: http://www.sensortips.com/temperature/designing-with-rtd-temperature-sensors/

A thermocouple is an electrical device consisting of two dissimilar conductors forming electrical junctions at different temperature. A thermocouple produces a temperature-dependent voltage because of the thermoelectric effect, and this voltage can be interpreted to measure temperature. Thermocouples are a widely-used type of temperature sensor. Commercial thermocouples are inexpensive and interchangeable and can measure a wide range of temperatures. These are self-powered and require no external form of excitations. Main problem related to thermocouples is its accuracy, system error of less than 1℃ can be difficult to achieve. Thermocouple life expectancy varies from few hours to few years, the many factors that contribute to determining life expectancy include calibration type, the environment, temperature, sensor design, and thermal cycling.

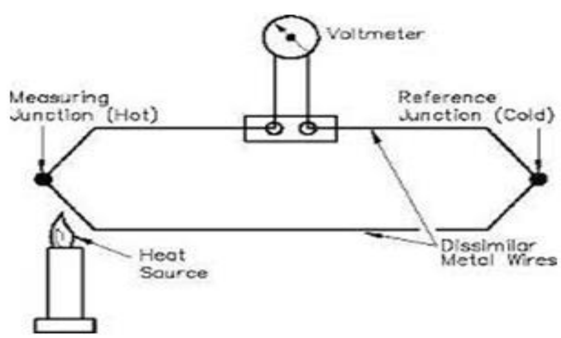

Figure 1.2: Thermocouple circuit.
Source: https://www.elprocus.com/temperature-sensors-types-working-operation/

The thermistors, are thermally sensitive resistors composed of metallic oxides of manganese, nickel, iron, cobalt and many more. They have a very high sensitivity towards small temperature changes. It has small mass and good thermal conductivity. It also has good long term stability and intrinsic roughness. The temperature of the thermistor is that of its surroundings. However, above specific current, current flow generates heat that make the temperature of the thermistor above the ambient temperature. Thermistors are among the most flexible transducer in common use. During the past decade, electronic thermometers based on thermistor sensors have become accepted tools within wide segments of the medical profession. Issues of using thermistors as sensors in biological systems is, it is nonlinear and has tendency for self-heating. Unfortunately, thermistors require more complicated software to account for their very nonlinear temperature response. The smart catheter temperature sensors are based with 4-probe wire configuration.

CHAPTER 2

INTRODUCTION OF SENSORS IN BIOLOGICAL SYSTEMS

2.1 What is Sensors?

Sensor is an electronic component whose purpose is to detect events or changes in its environment and send the information to the other electronics mostly a processor. A sensor's sensitivity indicates how much the sensor's output changes when the input quantity being measured changes. A sensor converts the physical parameter into a signal which can be measured electrically. The most common parameter measured is temperature. At present temperature is the only parameter covered in detail. Sensors are used in everyday objects such as touch-sensitive elevator buttons, lamps which switches off or on by touching its base. With advances in micromachinery and convenient microcontroller platforms, the uses of sensors have expanded beyond traditional fields. Sensors are usually designed to have small effect on what is measured making the sensor smaller often improves this and may introduce other advantages. Sensors used in temperature measurement have an electrical property that is sensitive to temperature changes. Since the range of the output signal is always limited, the output signal will eventually reach a minimum or maximum when the measured property exceeds the limits.

The full-scale range defines the maximum and minimum values of the measured property. The sensitivity may in practice differ from the value specified. This is called a sensitivity error. This is an error in the slope of a linear transfer function. If the output signal differs from the correct value by a constant, the sensor has an offset error or bias. This is an error in the y-intercept of a linear transfer function. Nonlinearity is deviation of a sensor's transfer function from a straight-line transfer function. Usually, this is denoted by the amount the output differs from ideal behavior over the full range of the sensor, often noted as a percentage of the full range. Rapid changes caused by the variation of the measured property over time is a dynamic error. Often, this behavior is described with a plot showing sensitivity error and phase shift as a function of the frequency of a periodic input signal. If the output signal slowly changes independent of the measured property, this is defined as drift. Long term deposit over months or years is caused by physical changes in the sensor. Noise is a random deviation of the signal that varies in time. A hysteresis error causes the output value to vary depending on the previous input values. If a sensor's output is different depending on whether a specific input value was reached by increasing vs. decreasing the input, then the sensor has a hysteresis error. If the sensor has a digital output, the output is essentially an approximation of the measured property. This error is also called quantization error. If the signal is monitored electronically, the sampling frequency can cause a dynamic error, or if the input variable or added noise changes periodically at a frequency near a multiple of the sampling rate, handling errors may occur. The sensor, to some extent be sensitive to properties other than the property being measured. For example, the temperature of their environment influences most sensors.

Measurement of temperature is critical in modern electronic devices, especially expensive laptop computers and other portable devices with densely packed circuits which dissipate considerable power in the form of heat. Knowledge of system temperature can also be used to control battery charging as well as prevent damage to expensive microprocessors. Compact high power portable equipment often has fan cooling to maintain junction temperatures at proper levels. To conserve battery life, the fan should only operate when necessary. Accurate control of the fan requires a knowledge of critical temperatures from the appropriate temperature sensor. Accurate temperature measurements are required in many other measurement systems such as process control and instrumentation applications. In most cases, because of low level nonlinear outputs, the sensor output must be properly conditioned and amplified before further processing can occur. Except for IC sensors, all temperature sensors have nonlinear transfer functions. In past, complex analog conditioning circuits were designed to correct for the sensor nonlinearity. These circuits often required manual calibration and precision resistors to achieve the desired accuracy. Today, however, high resolution ADCs may directly digitize sensor outputs. Linearization and calibration is then performed digitally, thereby reducing cost and complexity. Resistance Temperature Devices (RTDs) are accurate, but require excitation current and are generally used in bridge circuits. Thermistors have the most sensitivity but are the most non-linear. Nonetheless, they are popular in portable applications such as measurement of battery temperature and other critical temperatures in a system.

2.2 Different Types of Sensor

2.2.1 Temperature Sensors

Temperature is the most common of all physical measurements. We have temperature measurement and control units, called thermostats, in our home heating systems, refrigerators, air conditioners, and ovens. Temperature sensors are used on circuit boards, as part of thermal tests, in industrial controls, and in room controls such as in calibration labs and data centers. Though there are many types of temperature sensors, most are passive devices: Thermocouples, RTDs (resistance temperature detectors), and thermistors. Thermocouples (T/Cs) are the most common type of sensor because they don't require an excitation signal. They consist of two wires made of dissimilar metals joined at the point of measurement. Based on the Seebeck effect, T/Cs operate on the basis that each metal develops a voltage difference across its length based on the type of metal and the difference in temperature between the ends of the wire. By using two metals, we get two different voltages V_1 and V_2. The difference (V_T) represents temperature. Note that there is no voltage across the thermocouple junction. It is often heard that a thermocouple develops a voltage across the junction, which is incorrect. The voltage is developed over the length of each wire.

Thermocouples are designated using letters. A Type-J T/C has iron and constantan (a copper-nickel alloy) wires. Most thermocouple wire is color coded. Thermocouples require that the far ends of the wire be at the same temperature and that temperature must be known. Thus, instruments that use thermocouples will have an isothermal block with an embedded sensor to measure the temperature at that point. This is called cold-junction compensation. With one end of the wires at an equal and known temperature, a circuit can measure VT and calculate the unknown temperature. Thermocouple curves are nonlinear and hence require linearization. That can be done in hardware of software, mostly in software with today's digital instruments through an equation or reference table. Thermocouples are common because of their wide temperature range (type J can run up to 760°C), low cost, robustness, and simple signal-conditioning circuit. Wires can be run over long distances with proper shielding because the voltages are in microvolts/°C.

They're often used in industrial applications such as ovens and furnaces. Resistance-temperature detectors (RTDs) have a smaller range, typically a few hundred degrees Centigrade, but they have better accuracy and resolution than thermocouples. RTDs use precision wire, usually made of platinum, as the sense element. The element needs a known excitation current, typically 1mA. RTDs come in two-, three-, and four-wire configurations. Four-wire configurations, usually used as reference probes in calibration labs, have the best accuracy because two wires carry current and two are used for measuring the resistance across the element. RTDs are specified with a base resistance, typically 100.0Ω at 0°C for platinum wire, and a resistance slope. For example, a 385 Pt100 RTD has a slope of 0.00385Ω/Ω/°C from 0°C to 100°C. At 100°C, the resistance is 138.5Ω. For applications between 0°C and 100°C, RTDs may be considered linear. RTDs are often used in regulated industries such as food processing where the temperature ranges aren't as wide as for thermocouples, but a higher accuracy is needed. Because RTDs produce resistance as a function of temperature, the instrumentation often uses them in bridge circuits to maximize resolution. From there, the bridge output is digitized and linearized in software. Thermistors are also resistance-based temperature sensors, but their resistance/temperature curve has a negative slop and is highly nonlinear. But, they produce a higher change in resistance for a given change in temperature than RTDs. They're often used where the highest resolution is needed, though over a relatively narrow temperature range. Thus, thermistors are often used in medical devices, home thermostats, and machines. Engineers often use thermistors to measure temperature in circuit such as power supplies. Thermistors produce a significantly higher resistance than RTDs, typically 2000Ω to 10,000Ω. In a way, they can operate at a significantly smaller excitation current, which reduces loss in wires. So, thermistors are often used in two-wire circuits.

2.2.2 Pressure and Strain Sensors

Industrial and manufacturing systems rely heavily on pressure sensors and strain gages for the measurement and control of gases and weights. A company that produces gypsum wallboard (sheet rock) used strain gages in hoppers that would hold the gypsum powder. The hopper would vibrate to release the powder as needed for production. At an oil refinery, four tall storage tanks had a strain-gage sensor at the top and bottom of each tank. Each of the eight sensors connected to a data-acquisition system that calculated differential pressure between the sensors, converting each calculation into a 4-20mA signal for driving analog dials in a control room. In each case, the sensors connected to Wheatstone Bridge circuits in the instrumentation, which also provided excitation power for the sensors. A strain gage is typically made of a material that changes resistance when deformed, or put under strain. Because the change in resistance is small, these sensors are often connected in one segment of Wheatstone Bridge circuit where the other three resistances are known.

Pressure sensors, typically used to measure air, gas, or fluid pressure, are often designed using piezoelectric sensors or quartz sensors. Their analog outputs can be either voltage, such as 1-5V, or current, such as 4-20mA. The outputs can represent pressure in units of bars, kg/cm2, or PSI. Sensors are designed to measure either absolute pressure, relative to a vacuum, differential pressure--the pressure between two points, or gauge pressure, which is pressure relative to atmospheric conditions. While one may think of pressure sensors mainly for industrial use, other pressure measurements can take place in automotive, ergonomic, and other applications. For example, flexible pressure sensors, which are more like strain gauges, are used in designing products such as mattresses and automotive seats.[8]

2.2.3 Position Sensors

There was once a time when position sensors were used for detecting motion in industrial systems, aircraft, ships, and other large systems. Accelerometers, which measure motion in as many as three axes, were used to measure vibration in machines for predictive maintenance or in aircraft wings for test. Then something happened. Sensors became small and inexpensive enough to be used in consumer products. In recollection of visiting a company in the 1990s that was developing MEMS (microelectromechanical) accelerometers. In the lab, an engineer demonstrated how the device could be used in a game controller. That seemed incredible at the time but today, that's commonplace. Next, a company named after a fruit embedded accelerometers in phones and tablet computers, opening a huge market for these sensors. Accelerometers typically have internal piezoelectric devices that produce a voltage in response to motion. MEMS devices also respond to motion. You typically need an op-amp for signal conditioning before digitizing the sensor's output although many have signal-conditioning circuits built into the package and produce signals large enough for direct interfacing to digitizers. An accelerometer responds to a force applied to the sensor in the opposite direction.

2.2.4 Humidity Sensors

Many environmental tests performed as part of product characterizations rely on testing over a range of humidity. After all, many products must work in the deserts of Arizona to forests of New England. Humidity measurements are also use in applications such as aviation, weather, and scientific applications. Our home appliances have become smarter; humidity sensors have found their way into white goods such as refrigerators. During the heating season, sensor uses a capacitive technology where the capacitive value changes with humidity. It's another application of sensing capacitance, which we discussed regarding touch-screen technology. A humidity tutorial from Vaisala shows that humidity instruments started as mechanical devices that used horse hair. As technology improved, the wet/dry bulb became popular. Next came the chilled mirror, which used light that reflected in a wider pattern in the presence of dew. When electrical humidity sensors entered the scene, they started as resistive devices but have now become capacitive. Early capacitive sensors used aluminum oxide (AL_2O_3) but have since moved to polymer based technologies.

2.2.5 Light Sensing

There are many ways to detect light using electronic components. Every cell phone and digital camera has a light-sensing array for taking photos. Engineers use other light-sensitive components such as photo resistors, photodiodes, and photodetector ICs in all kinds of applications. Photodiodes are particularly useful as detectors of light in fiber-optic networks. Over the years, engineers have contributed many circuits to EDN Design Ideas that use photosensitive devices. Photo resistors are used when you need a resistive analog response to a light level. Photodiodes are both digital devices and analog devices. As digital devices, they turn on and off when they sense a given level of light. Analog photodiodes produce an analog quantity based on received light. You can use these sensors in applications such as circuit to control relays and timers.

Device	Photo resistor	Photo diode	Photo transistor	Photo diode and current amplifier	Photo diode, current amp, ADC and filter
Referenced part #	PDV-P500X	Everlight DTD-15	Everlight DPT-092	EL7900	ISL29001
	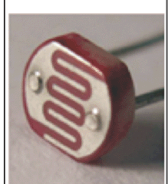	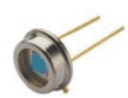		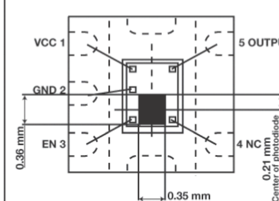	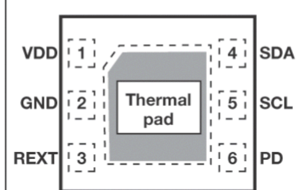
Accuracy	Not guaranteed	Not guaranteed	± 75%	± 33%	15-bit resolution
Current (1000 lux)	Varies	3 μA	2.6 mA (70 klux)	0.9 mA	0.3 mA
Range	1 to 100 lux	7 to 50 klux	1 k to 100 klux	1 to 100 klux	0.3 to 10 klux
Response time	55 ms	6 ns	15 μs	0.5 ms	100 ms
Enable function	No	No	No	Yes	Yes

Figure 2.1 Types of different light sensors.

Source http://www.eetimes.com/document.asp?doc_id=1272314

2.2.6 Sound and Vibration Sensing

Sound and vibration sensing is a subset of the accelerometers previously covered. Many machines vibrate during use and may make noise, both of which need to be measured and analyzed. A typical example is a washing machine. When not evenly balanced, it can vibrate excessively. As part of the test and qualification process, engineers will monitor the vibrations and noise of such products. Sensors such as accelerometers, combined with data-acquisition equipment and specialized software, let you analyze the vibrations. MEMS-based microphones are often used in sound capture and analysis. Analog and digital MEMS microphone design considerations from EE Times explains how MEMS microphones work and what kind of signal-conditioning circuits they need. For example, you need a high-impedance input stage following the MEMS microphone because of its typical 200Ω output impedance. MEMS digital microphones integrate an ADC into the sensor, providing direct digital output in I 2S (inter-IC sound) and PDM (pulse-density modulation) formats. You can connect them directly to microcontrollers. Digital microphones are often used in smart phones, tablet computers, laptops computers, headphones (for noise cancellation) and hearing aids. Going a step further, researchers at the University of Utah developed a MEMS microphone that can be implanted in the middle ear.

2.2.7 Capacitive Sensing

Sensing capacitance took on a whole new meaning with touch screens, particularly with the iPhone and iPad became popular. Capacitive sensing began its life long before the iPhone, having been used to detect fluid levels, humidity, and material properties. Capacitive sensors are typically made of several layers of materials, often on a circuit board. In touch-screen or button applications, a sensor IC detects not absolute capacitance, but a change in capacitance, indicating the location of your finger. Because these screens rely on the change in capacitance based on your skin, they don’t work with your fingernails. The figure below (courtesy of Texas Instruments) shows an equivalent circuit for a touch screen. With capacitive sensing, your finger is never in contact with the sensing device. Thus, there's no mechanical wear (unless you break the screen on your phone). Your finger interferes with a local electric field, which changes capacitance and is sensed by an IC, digitized, and sent to a microcontroller. The capacitive-sensing IC produces an excitation signal that creates the local electric field in the sensing surface.

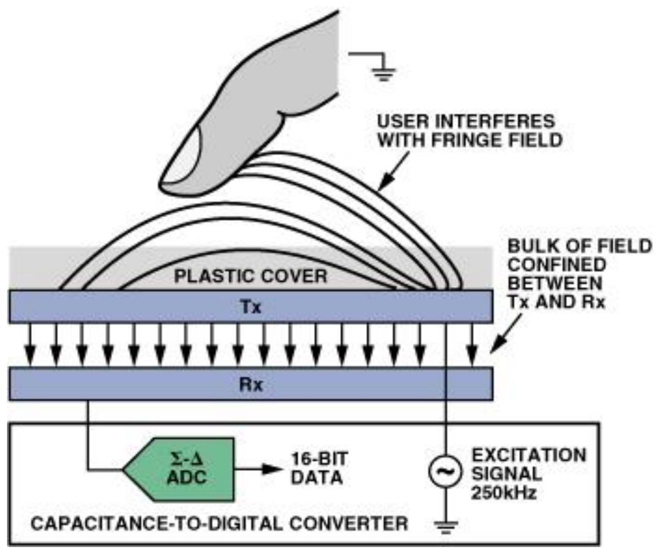

Figure 2.2 A capacitive sensing**.**
Source http://www.analog.com/en/analog-dialogue/articles/capacitance-sensors-for-human-interfaces-to-electronics.html

A capacitive sensing IC scans the buttons or screen locations. Thus, there can be timing issues between when a change in capacitance occurs and when the IC scans that location. Because a scan occurs for a fixed amount of time at each location, the sensing IC applies a counter to the charge time of a known capacitor. Changes in the total capacitance (accounting for the touch or lack of touch) cause a counter to create a number proportional to current. It's essentially an integration process. If the count exceeds a specific value, the circuit interprets that as a touch and the system acts upon that event.

2.2.8 Optical Fiber Sensor

A sensor that measures a physical quantity based on its modulation on the intensity, spectrum, phase, or polarization of light traveling through an optical fiber. An optical sensor is a device that converts light rays into electronic signals. Like a photo resistor, it measures the physical quantity of light and translates it into a form read by the instrument. Optical sensors have a variety of uses. They can be found in everything from computers to motion detectors. For example, when the door to a completely darkened area such as the inside of a copy machine is opened, light impacts the sensor, causing an increase in electrical productivity. This will trigger an electric response and stop the machine for safety. distinction is often made in the case of fiber sensors as to whether measure and act externally or internally to the fiber. Where the transducers are external to the fiber and the fiber merely registers, and transmits the sensed quantity, the sensors are termed extrinsic sensors. Where the sensors are embedded in or are part of the fiber and for this type there is often some modification to the fiber itself the sensors are termed internal or intrinsic sensors.

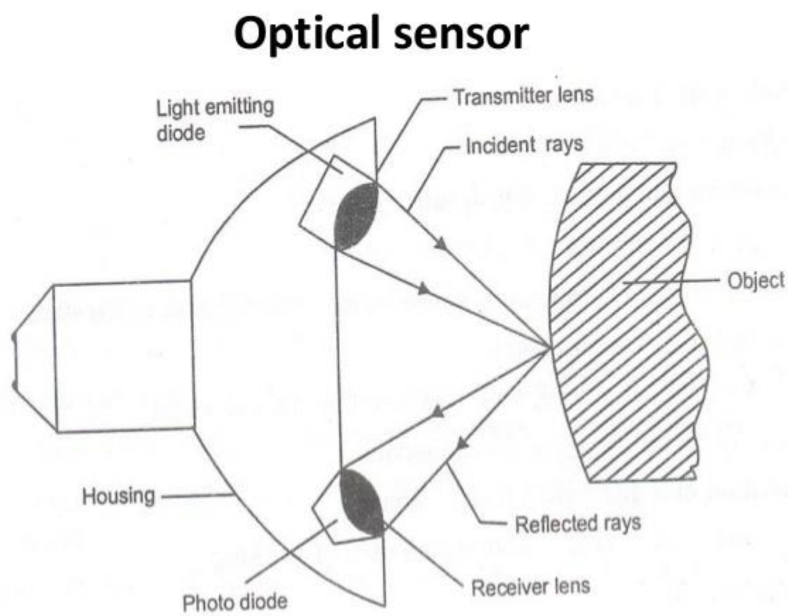

Figure 2.3 An optical sensor.
Source https://www.slideshare.net/satyanaveenvyas/proximity-sensors.

2.2.9 Infrared Sensors

Infrared waves are not visible to the human eye. In the electromagnetic spectrum, infrared radiation can be found between the visible and microwave regions. The infrared waves typically have wavelengths between 0.75 and 1000µm. The wavelength region which ranges from 0.75 to 3µm is known as the near infrared regions. The region between 3 and 6µm is known as the mid-infrared and infrared radiation which has a wavelength greater higher than 6µm is known as far infrared. There are mainly two types of Infrared sensors: Thermal infrared sensors – use infrared energy as heat. Their photo sensitivity is independent of the wavelength being detected. Thermal detectors do not require cooling but do have slow response times and low detection capabilities. Quantum infrared sensors – provide higher detection performance and faster response speed. Their photo sensitivity is dependent on wavelength. Quantum detectors must be cooled to obtain accurate measurements. All objects which have a temperature greater than absolute zero (0 Kelvin) posses thermal energy and are sources of infrared radiation as a result. Sources of infrared radiation include blackbody radiators, tungsten lamps and silicon carbide. Infrared sensors typically use infrared lasers and LEDs with specific infrared wavelengths as sources. A transmission medium is required for infrared transmission, which can be comprised of either a vacuum, the atmosphere or an optical fiber.

Figure 2.4 The image of a house under infrared sensor.
Source http://www.azosensors.com/article.aspx?ArticleID=339#

Optical components, such as optical lenses made from quartz, CaF_2, Ge and Si, polyethylene Fresnel lenses and Al or Au mirrors, are used to converge or focus the infrared radiation. To limit spectral response, band-pass filters can be used. Infrared detectors are used to detect the radiation which has been focused. The output from the detector is usually very small and hence pre-amplifiers coupled with circuitry are required to further process the received signals

2.3 It's Usage

In our day-to-day life we frequently use different types of sensors in several applications such as IR sensor used for operating television remote, Passive Infrared sensor used for automatic door opening system of shopping malls and LDR sensor used for outdoor lighting or street lighting system.

2.3.1 Temperature Sensors

Design of Industrial Temperature Controller for controlling temperature of devices used in industrial applications is one of the frequently used practical applications of the temperature sensor. In this circuit, IC DS1621, a digital thermometer is used as a temperature sensor, thermostat, which provides 9-bit temperature readings. The circuit mainly consists of 8051 microcontroller, EEPROM, temperature sensor, LCD display and other components. LCD is used to display temperature in the range of -55degress to +125degrees. EEPROM is used to store predefined temperature settings by user through the 8051-series microcontroller. The relay whose contact is used for load, is driven by microcontroller using a transistor driver.

2.3.2 IR Sensors

Thermography – According to the black body radiation law, it is possible to view the environment with or without visible illumination using thermography. Heating – Infrared can be used to cook and heat food items. They can take away ice from the wings of an aircraft. They are popular in industrial field such as, print dying, forming plastics, and plastic welding. Spectroscopy this technique is used to identify the molecules by analyzing the constituent bonds. This technique uses light radiation to study organic compounds. Meteorology Cloud heights, calculate land and surface temperature is possible when weather satellites are equipped with scanning radiometers. Photobiomodulation – This is used for chemotherapy in cancer patients. This is used to treat anti herpes virus. Climatology – Monitoring the energy exchange between the atmosphere and earth. Communications – Infra red laser provide light for optical fiber communication. These radiations are also used for short range communications among mobiles and computer peripherals.

2.3.3 Pressure Sensors

This is where the measurement of interest is pressure, expressed as a force per unit area. This is useful in weather instrumentation, aircraft, automobiles, and any other machinery that has pressure functionality implemented. This is the use of pressure sensors in conjunction with the venturi effect to measure flow. Differential pressure is measured between two segments of a venturi tube that have a different aperture. The pressure difference between the two segments is directly proportional to the flow rate through the venturi tube. A low-pressure sensor is almost always required as the pressure difference is relatively small. A pressure sensor may also be used to calculate the level of a fluid. This technique is commonly employed to measure the depth of a submerged body (such as a diver or submarine), or level of contents in a tank (such as in a water tower). For most practical purposes, fluid level is directly proportional to pressure. In the case of fresh water where the contents are under atmospheric pressure, 1psi = 27.7 inH20 / 1Pa = 9.81 mmH20.

.

2.3.4 Fiber Optic Sensors

These are used in several areas. Specifically Measurement of physical properties such as strain, displacement, temperature, pressure, velocity, and acceleration in structures of any shape or size. Monitoring the physical health of structures in real time. Buildings and Bridges: Concrete monitoring during setting, crack (length, propagation speed) monitoring, pre-stressing monitoring, spatial displacement measurement, neutral axis evolution, long-term deformation (creep and shrinkage) monitoring, concrete-steel interaction, and post-seismic damage evaluation. Tunnels: Multipoint optical extensometers, convergence monitoring, shotcrete / prefabricated vaults evaluation, and joints monitoring damage detection. Dams: Foundation monitoring, joint expansion monitoring, spatial displacement measurement, leakage monitoring, and distributed temperature monitoring. Heritage structures: Displacement monitoring, crack opening analysis, post-seismic damage evaluation, restoration monitoring, and old-new interaction.

CHAPTER 3

PRINCIPLE OF OPERATION

3.1 Design and Fabrication

Coming back to the smart polymeric temperature sensors. Biomedical microdevices have been used in the clinical setting for quite some time and are instrumental to the delivery of care. Recent developments in microelectromechanical systems (MEMS)-based sensors prefer that the quality of diagnosis and treatment can be significantly enhanced once these advancements are translated into the targeted applications[2]. MEMS-based sensors have advantages over traditional monitoring probes include smaller dimension, ability to integrate, faster response time, lower power consumption, lower cost, greater reliability and higher sensitivity. In addition, the advancement in fabricating the MEMS sensors on a flexible substrate offers a viable solution to one of key technical challenges of rigid monitoring probes the mechanical mismatch between the compliant brain tissue and the sensor substrate. A smart catheter was developed, which is capable of continuously monitoring multiple physiological and metabolic parameters.

Microsensors, wires and circuits were fabricated first on the flexible polymer substrate using standard MEMS technology, and then rolled spirally to make a tube structure. It combined the advantages of flexible MEMS technology with a spiral rolling technique to develop a multimodality probe applicable to monitoring TBI patients, while avoiding wiring and assembling problems associated with previous methods. Furthermore, catheter lumen patency is maintained for *in situ* drug delivery, insertion of medical tools, or drainage of cerebrospinal fluid (CSF) or blood. For use in multimodality neuromonitoring with the smart catheter, it has evaluated the performance, accuracy and long-term stability of smart catheter temperature sensor (SCT) based on thin-film resistance temperature detector (RTD) with 4-wire configuration.

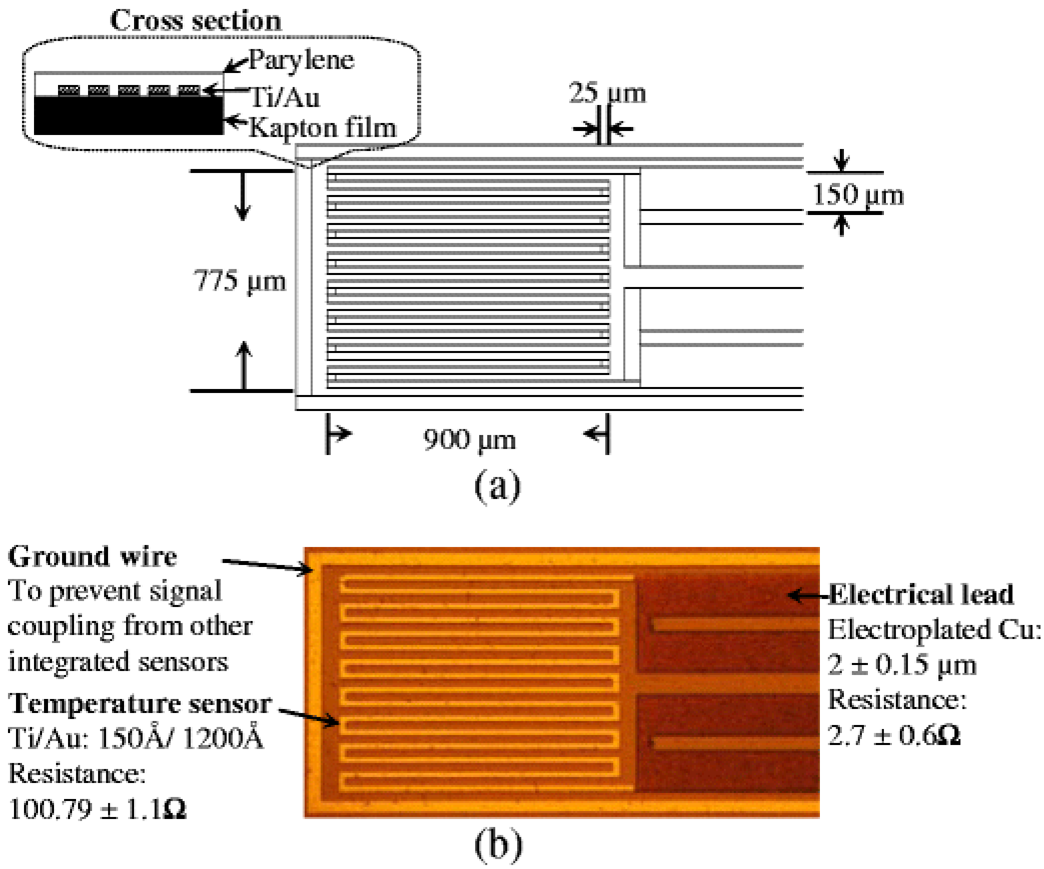

Figure 3.1 Smart catheter temperature sensor (SCT) with 4-wire resistance temperature detector (RTD) configuration: (**a**) SCT geometry and detailed dimensions and (**b**) photograph of microfabricated SCT.

Source Li, C., Wu, P., Wu, Z., Ahn, C. H., Ledoux, D., Shutter, L. A., . . . Narayan, R. K. (2011). Brain temperature measurement: A study of in vitro accuracy and stability of smart catheter temperature sensors. Biomedical Microdevices,14(1), 109-118. doi:10.1007/s10544-011-9589-4

The smart catheter flow sensor (SCF) consists of two components: a temperature sensor (SCT) which is located outside the "thermal influence" area for temperature compensation and a flow sensor which is heated 2°C above the medium temperature. Both temperature and flow sensors use a 4-wire configuration to eliminate the effect of lead wires. The SCF operates in a constant-temperature mode and employs a periodic heating and cooling technique[7]. the operation procedures are described as follows. First, a very small amount of current inducing self-heating is applied to the sensor followed by measurement of the "cool" sensor resistance. The overheating resistance can then be determined by multiplying the "cool" sensor resistance by a factor depending on the desirable sensor overheating temperature, a feedback loop is initiated and sustained by repeating the following steps: measure the sensor resistance, compare it with the overheating resistance, and then increase or decrease the applied current according to the comparison results.

At the steady-state, the current applied to the sensor settles to a constant leading to the constant temperature condition. However, the applied current varies whenever the sensor is subject to different flow rates. The current tends to increase as the flow rate increases and correlates linearly with the flow rate within a certain range. The working principle mentioned above implies that the outputs will still be affected by two factors. One is the medium temperature change during the heating period[1]. To compensate for the change occurring within a single period, a SCT is used to provide the medium temperature data to the SCF so that the overheating resistance can be adjusted while the sensor is in its heating state. The other is the effect of thermal conductivity because the output is also a function of thermal conductivity of the sensor and its adjacent medium. In real application, the thermal conductivity of the medium is not a constant. In our approach, two sets of data points are taken in a single heating period to realize thermal conductivity compensation.

The first set consists of the peak output related to the intrinsic property of the medium and the second is the steady-state output related to the flow rate. The thermal conductivity compensation is performed to the first order using the two data sets.

The temperature sensor is designed primarily for the smart catheter, which is capable of multimodality neuromonitoring. A RTD is used as the temperature sensor, which is one of the most accurate temperature sensors. As a metal conductor with a positive temperature coefficient (PTC), the resistance of RTD increases proportionally with an increasing environmental temperature in the linear range. With the advent of microfabrication technology, RTD temperature sensors can be made from thin-film metal. The advantages of a thin-film RTD temperature sensor are small volume, high accuracy, short response time, suitability for mass production, and ability to measure temperature more precisely than a traditional thermocouple[1]. Thin-film RTD also exhibits superior specifications over the thermistor in terms of linearity, long-term stability, interchangeability. Measuring the RTD with 4-wire setup yields the most accurate output since the method not only cancels the lead wire effect but the effect of mismatched resistances from contact points. Commonly used sensing materials in temperature sensors are Pt and Au particularly, Pt is more expensive, and Au has comparable temperature coefficient of resistance and flexibility. Therefore, Au with a 4-wire configuration is used for the smart catheter in this work. The resistance of a general metal is expressed as where R is resistance (Ω); ρ is resistivity (Ω_m); L is resistor length (m) and A is cross-sectional area (m_2).

$$R=\rho\frac{L}{A} \tag{3.1}$$

The electrodes have twisting micro temperature sensor structures, with a sensing area of 775 μm×900 μm. As the temperature of the RTD varies, the nearly linear relationship between measured resistance and change in temperature can be expressed as follows:

$$R_t = R_i(1 + \alpha t) \tag{3.2}$$

$$\Delta T = t + i \tag{3.3}$$

where R_t and R_i are the resistance of an RTD at t (°C) and I (°C), respectively; αT is the positive temperature coefficient of an RTD (1/°C); and ΔT is the deviation in temperature from the reference temperature. Therefore, Eq. 3.2 can be rewritten as,

$$\propto_T = \frac{R_t - R_i}{R_i(\Delta t)} \tag{3.4}$$

where α_T is the temperature coefficient of resistance (TCR) of a sensor.

The device fabrication is shown in the figure below. The flow and temperature sensor microelectrodes were fabricated by depositing a Au (1200Å) layer with an adhesion layer of Ti (150Å) on the 7.5μm thick Kapton film with 1μm Parylene film coating, followed by standard thin film lithography and etching processes. After that, the electrical leads of the flow and temperature sensors were electroplated with 2μm thick Cu to reduce the lead resistances. The levels with temperature sensor and flow sensor were separated by Parylene/Copper/Parylene (2μm/1200Å/2μm) layers to prevent noise coupling. Finally, 5μm thick Parylene film was deposited as a biocompatible and insulation layer. The film with microsensors were cut into size and spirally rolled over the metal rode based on our previous work to form an intraventricular catheter.

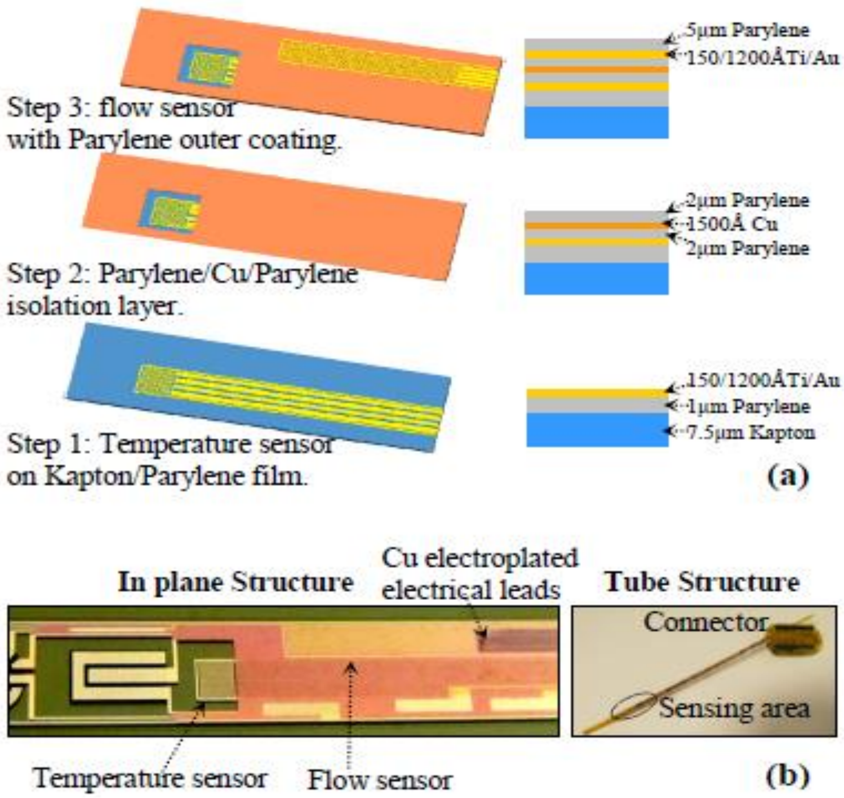

Figure 3.2 Microfabricated smart catheter flow sensor (a) schematic illustration of microfabrication procedure and (b) photographs of developed smart catheter with flow sensor

Source . Li, C., Wu, P., Wu, Z., Ahn, C. H., Ledoux, D., Shutter, L. A., . . . Narayan, R. K. (2011). Brain temperature measurement: A study of in vitro accuracy and stability of smart catheter temperature sensors. Biomedical Microdevices,14(1), 109-118. doi:10.1007/s10544-011-9589-4

3.2 Working Principle

The four-wire principle and coordinated detection method were to obtain an accurate sensor signal. Four wire configuration excludes the effect of the lead wire. Synchronous detection can prevent dc shift caused by the thermoelectric effect induced on the dissimilar metal junctions. The simplified circuit is illustrated in Figure 3.3 where (a) is the excitation circuit, (b) the readout circuit, (c) the isolation circuit and (d) the calibration circuit. Circuit (a) and (b) are essential for sensor operation. Digital isolator circuit (c) is included to prevent its analog ground being interfered by the ground noise of the back-end circuit. The use of digital-to-analog converter (DAC) is optional, though its addition allows direct readout of the sensor analog outputs using a multimeter. This makes it convenient for troubleshooting. The calibration circuit (d) provides an interface for the user to perform sensor calibration.

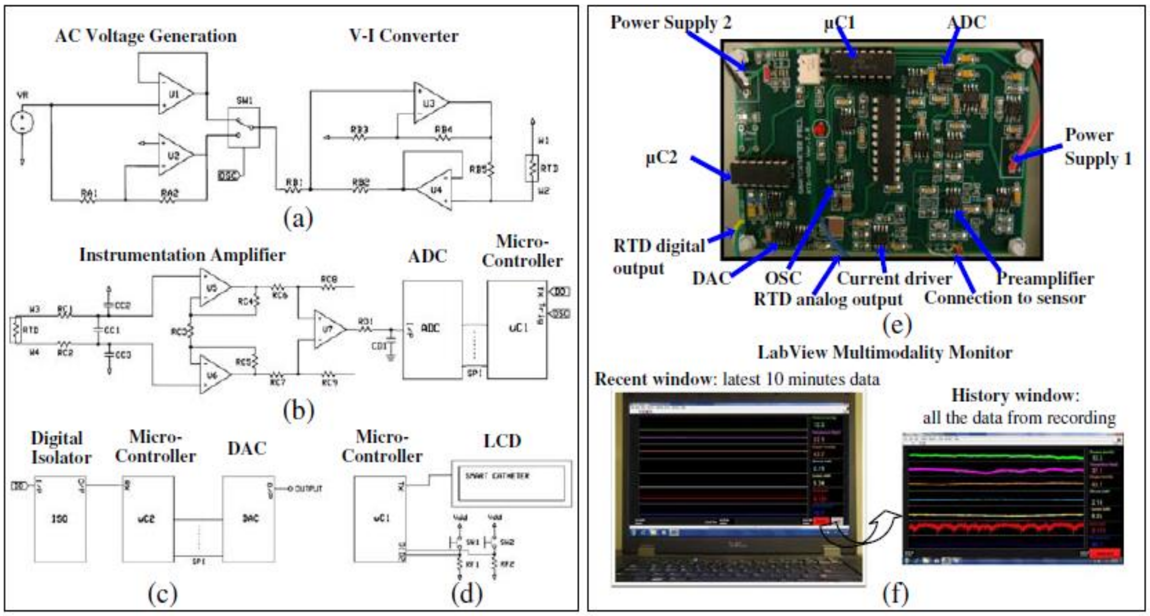

Figure 3.3 :- Prototyped temperature sensing circuit and monitor: (a) schematic layout of excitation circuit section; (b) readout circuit section; (c) isolation circuit section; (d) calibration circuit section; (e) photograph of developed SCT circuit and (f) photograph of developed LabView multimodality monitor.

Source:- Li, C., Wu, P., Wu, Z., Ahn, C. H., Ledoux, D., Shutter, L. A., . . . Narayan, R. K. (2011). Brain temperature measurement: A study of in vitro accuracy and stability of smart catheter temperature sensors. Biomedical Microdevices,14(1), 109-118. doi:10.1007/s10544-011-9589-4

The lactate biosensor was designed for long-term accurate and stable *in vivo* monitoring. For insertion applications, amperometric enzyme-based biosensors are currently superior to other sensor types due to the high selectivity of enzymes. Most *in vivo* biosensors rely on mediator less-based detection of hydrogen peroxide (H_2O_2) due to potential leaching and toxicity of the mediator. Lactate oxidase (LOD)-based biosensors are the most widely used configuration and allow the determination of H_2O_2 generated in the enzymatic reaction. LOD catalyzes the oxidation of lactate to pyruvate. In the presence of dissolved O_2, the enzyme can be re-oxidized, releasing H_2O_2. The produced H_2O_2 can be oxidized at the electrode surface giving a current proportional to the amount of dissolved lactate. In spite of its specificity, LOD-based biosensors suffer from some limitations, such as short stability and oxygen and temperature dependency. LOD, the enzyme used in the construction of the lactate biosensor, is known to be quite unstable with respect to enzymatic activity over time. This leads to reduced sensor lifetimes[11]. To enhance the biosensor's stability and lifetime, besides immobilizing the LOD in the optimized conditions (temperature, pH, and curing agent concentration) to provide a favorable micro-environment, a novel groove structure has been developed between the working and counter electrodes to store excess enzymes[6]. To solve the issue of temperature dependency, a combination of a temperature sensor to do *in situ* temperature compensation using the following equation:

$$I_{CT} = I_t + (I_t \times F_T)(T_{25} - T_t) \quad (3.5)$$

where I_{CT} is the compensated current for temperature dependency of lactate biosensor (nA), Tt is the measured temperature at the time t by the temperature sensor (°C), F_T is the temperature factor system (%/°C), and It is the current measured at the time t during the experiments (nA). Automatic temperature dependency correction for the lactate biosensor was performed, we coated the sensor with poly (vinyl alcohol) (PVA) hydrogels. PVA hydrogels have the oxygen-storing capability due to the formation of larger hydrophobic domains during the freeze-thaw (F_T) cycles.

The temperature sensor operates with AC excitation current of 500 μA and updates its outputs every 200 ms. Its output voltage is derived as follows:

$$V_0 = [\, V_r(1 + \alpha * \Delta T_{t1} + V_{n1}] - [\, V_r(1 + \alpha * \Delta T_{t2} + V_{n2}] \qquad (3.6)$$

where V_0 is the final voltage output, α is the temperature coefficient (TCR) of a RTD, V_r is the voltage output at a reference temperature (°C), ΔT_{t1} and ΔT_{t2} is the deviation in temperature from the reference temperature at time t1 and t2, and ΔV_{n1} and ΔV_{n2} represent the voltage offset caused by the thermal electric effect. For fast excitation, it is reasonable to assume that $\Delta T_{t1} = \Delta T_{t2} = \Delta T$ and $\Delta V_{n1} = \Delta V_{n2}$.

Thus, the equation can be further reduced to:

$$V_0 = 2V_r(1 + \alpha * \Delta T) \qquad (3.7)$$

Define ΔT_{0T} - T_r, where T is the measured temperature and T_r is the reference temperature. Rearranging the equation gives the measured temperature:

$$\mathrm{T} = \mathrm{T_r} + \frac{\frac{\mathrm{V_0}}{2\mathrm{V_r}} - 1}{\alpha} \qquad (3.8)$$

The flow sensor employs a periodic heating and cooling technique under a constant-temperature mode and updates its outputs every 10 s. During the cooling period, the flow sensor is cooled down to the medium baseline temperature and the heating period is held 2.5 °C above the medium temperature. The detailed operation can be categorized into five regions as shown in figure below.

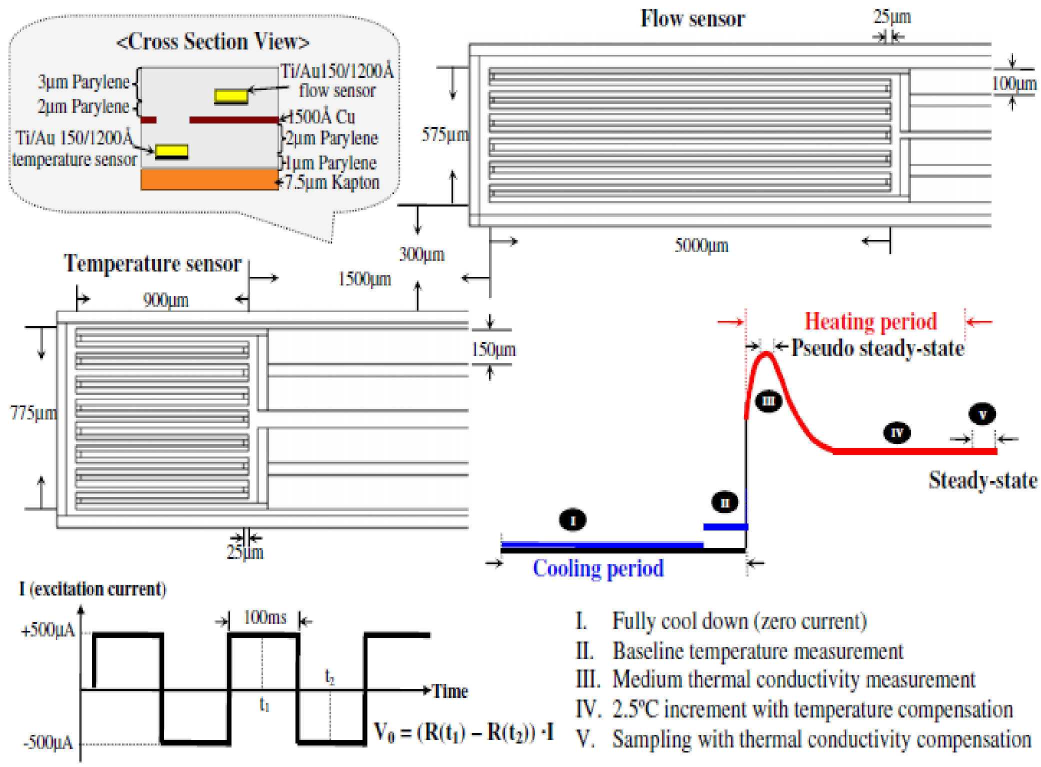

Figure 3.4 Micromachined lab-on-a-tube (LOT) with brain temperature sensor and cerebral blood flow sensor: Temperature sensor with 4-wire resistance temperature detector (RTD) configuration operates with ac excitation current of 500 µA and updates its outputs every 200 ms.
Source Li, C., Wu, P., Hartings, J. A., Wu, Z., Cheyuo, C., Wang, P., . . . Narayan, R. K. (2012). Micromachined lab-on-a-tube sensors for simultaneous brain temperature and cerebral blood flow measurements. Biomedical Microdevices,14(4), 759-768. doi:10.1007/s10544-012-9646-7

The cooling period consists of regions I and II and the heating period covers regions III, IV, and V. In region I, no current is applied and the sensor is cooled down from previous heating period. In region II, after the sensor settles to the medium temperature, a small current (500 µA) is applied, the sensor resistance is measured, and the overheating resistance is calculated. In region III, the circuit initiates the feedback control, thereby inducing an overshoot during heating the sensor. The peak output is sampled for use in the thermal conductivity compensation. The output then settles down to a stable value in region IV. During the heating period, medium temperature compensation is achieved by adjusting the overheating resistance according to the temperature sensor output. The end of region IV when steady state is achieved is defined as region V. Here, multiple data points are sampled and their average represents the flow rate without thermal conductivity compensation. The output without thermal conductivity compensation correlates to the flow rate using the simplified equation

$$V_f = C + D * F^n \tag{3.9}$$

where V_f is the uncompensated voltage output, C and D are coefficients related to conduction and convection, F is the flow rate and n is the fitting factor. The flow rate will be further processed with medium thermal conductivity compensation using the information from region III.

3.3 Materials Used

Standard microfabrication processes were used for development of the first-generation neural catheter Lactate sensor. Concisely, the polyimide PI2611 was spin-coated silicon wafer. The polyimide was cured under nitrogen atmosphere in a programmable oven at 400 °C for 30 min with a ramp rate of 4 °C/min to minimize thermal stress. After curing, a thin PI2611 film with thickness of 7 μm was obtained. After exposure to oxygen plasma for 30 s, a metal layer (Ti/Au 120 Å/1200 Å) was deposited using e-beam metal evaporator and patterned by photolithography to build the microelectrodes, interconnection lines and connection pads. A second PI2611 layer was then spin-coated to form a 7 μm thick passivation layer to insulate the interconnection lines. The cured second polyimide layer was etched in oxygen plasma for 10 min[14].

This etching step opened the microelectrodes and connection pads. Platinum nanoparticles were electrochemically deposited on all of the opened microelectrodes by cyclic voltammetry in 0.5 M H_2SO_4 solution containing 1.5 mM K_2PtCl_6 with cycling between 0.2 V and – 0.5 V at 55 mV/s Iridium oxide was further electrochemically deposited onto the Pt modified microelectrodes (reference electrodes for the ECoG and oxygen sensors; and ECoG recording electrodes) by cycling between 0 V and 0.6 V at 50 mV/s in the plating solution After that, the working electrode for the oxygen sensor was electro-coated in phosphate buffer pH 7.4 containing 300 mM o-phenylenediamine (oPD) solution by applying a potential of 0.7 V for 10 min. The flexible polyimide film was cut to size and spirally rolled to form a single neural catheter (inner diameter = 0.65 mm; outer diameter = 0.7 mm). 32-position male rectangular connector was bonded to the microsensor contact pads with silver paste and then covered with insulating epoxy. The in-plane structure and assembled neural catheter.

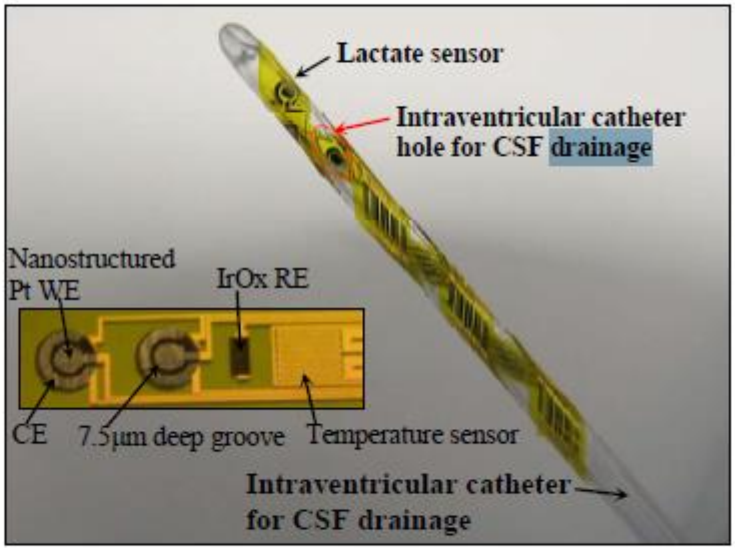

Figure 3.5 Lactate biosensors were spirally rolled outside an intraventricular catheter (6 French) without blocking the holes for CSF drainage. This structure ensures continuous CSF lactate measurements even with catheter occlusion.
Source Li, C., & Narayan, R. K. (2012). Development of a novel catheter for early diagnosis of bacterial meningitis caused by the ventricular drain. 2012 IEEE 25th International Conference on Micro Electro Mechanical Systems (MEMS). doi:10.1109/memsys.2012.6170108

For the catheter temperature sensor Polydimethylsiloxane (PDMS) was spin-coated on a 6-inch Silicon wafer and cured at 65 °C for 1 h. A 7.5 μm thick Kapton film (type HN) was cleaned and attached to the PDMS surface. 1.5 μm thick Parylene film was to smooth the film surface and enhance the resistance to moisture transmission. Electrodes for the temperature sensor were fabricated by depositing and patterning an Au (1,200 Å) layer with an adhesion layer of Ti (150 Å) using an E-beam evaporator, followed by standard lithography and etching processes.

After that, the electrical leads of the temperature sensor were electroplated with 2 μm thick Cu to reduce the lead resistances. Then 2 μm Parylene, 1,500 Å Cu, and 2 μm

Parylene were deposited in sequence to prepare the surface to develop the flow sensor. The electrodes for the flow sensor were fabricated by depositing and patterning the 150 Å Ti /1200 Å Au layers. The electrical leads of the flow sensor were also electroplated with 2 μm thick Cu to reduce the lead resistances. Finally, 3 μm thick Parylene film was deposited as an outermost layer. The film with the temperature and flow sensors were cut into size and spirally rolled over the metal rode based on our previous work to form an intraventricular. The film with temperature and other microsensors were cut into size (width=2.5 mm; length=150 mm) and spirally rolled over the metal rode based on our previous work to form an intraventricular catheter. The smart catheter was designed to have the same inner diameter (ID= 1.3 mm) as the Codman intraventricular catheter for compatibility with existing ventricular drainage techniques. After spiral-rolling, a post treatment is performed to enhance stability and durability. SCTs were electrified for aging with a 20 mA current for 12 h based on self-heating. Through the post treatments, the structural defects and internal stress are eliminated, and accordingly, the stability and TCR of the SCTs are enhanced. Each SCT was then calibrated.

CHAPTER 4

PRESENT STATUS OF THE SENSORS

A variety of new strategies have been developed toward biosensors with clinical applications. In principle, biosensors are analytical devices composed of a biological recognition element and an optical/electronic transducer. The biological element is in charge of capturing analytes in solution and the transducer converts the binding event to a measurable signal variation. The type of biosensors can be categorized by the nature of recognition, that is, enzyme-based biosensors, immunological biosensors, and DNA biosensors. Alternatively, based upon the type of transducers, there are electronic biosensors (electrical or electrochemical) , optical biosensors (fluorescent, surface plasmon resonance, or Raman) , and piezoelectric biosensors (quartz crystal microbalance).

Environmental monitoring is another important aspect wherein biosensor technology is required for rapid identification of pesticidal residues to prevent health hazards. Traditional methods, such as high-performance liquid chromatography, capillary electrophoresis and mass spectrometry, are effective for the analysis of pesticides in the environment yet, there are limitations for instance complexity, time-consuming procedures, requirement of high-end instruments, and operational capabilities. Hence, simple biosensors seem to have tremendous advantages yet, it is cumbersome to develop unified one for analyzing various classes of pesticides.

The incorporation of gold nanoparticles or quantum dots with the use of micro-fabrication provides new technology for the development of highly sensitive and portable cytochrome P450 enzyme biosensors for certain purpose. Furthermore, fiber-optic chemical sensors have lot of relevance in various fields, such as drug discovery, biosensing, and biomedicine. More recently, hydrogels, used as DNA-based sensor, are emerging materials for immobilization usage with fiber-optic chemistry. Compared to other materials, immobilization in hydrogels occurs in 3D which allows high loading capacity of sensing molecules. Hydrogels (polyacrylamide) are hydrophilic cross-linked polymers and can be made into different forms for immobilization ranging from thin films to nanoparticles.

If both chain ends were labeled with fluorescent donor and acceptor, the principle of Forster resonance energy transfer (FRET) can be employed for thermal sensing. It should be noted that the same strategy has been conventionally employed in protein and DNA folding studies. The chain ends of PNIPAM were labeled with pyrene and C60. Thermoinduced collapse of Py-PNIPAMC60 chain leads to decreased spatial distance between fluorescent pyrene dyes and the C60 quencher; i.e., enhanced FRET process can be achieved above the LCST. Thus, temperature changes can be transformed into fluorescence intensity changes due to enhanced or weakened fluorescence quenching efficiency at temperatures above or below the LCST.

Recently, the construction of a colorimetric and fluorometric temperature sensor based on organic/inorganic hybrid PNIPAM brushes. Consecutive ATRP copolymerization of NIPAM with specific fluorescent dyes from the surface of silica nanoparticles leads to hybrid nanoparticles coated with PNIPAM brushes of two layers, with the inner and outer layer covalently labeled with NBDAE and SP moieties. Under visible light, the outer layer is non-emissive.

Heating the aqueous dispersion of hybrid nanoparticles leads to the collapse of PNIPAM brushes, supplemented by an enhanced fluorescence emission from NBDAE moieties. Under UV irradiation, a ratiometric thermal sensor can be constructed based on the FRET process between NBDAE (fluorescence donor) in the inner layer and ring-opened MC form of SP (fluorescence acceptor) in the outer layer. On heating, the collapse of PNIPAM brush leads to decreased spatial distances between fluorescent donors and acceptors, i.e., enhanced FRET efficiency. Within the temperature range of 20-40℃on UV irradiation, a colorimetric yellow-to-red transition can also be determined by the naked eye. Because of their unique photoluminescence behavior of quantum dots i.e., size-tunable emission color, narrow and symmetric emission profile, and high emission stability against bleaching, they have also been integrated into thermo-responsive PNIPAM microgels to construct thermal sensors. There are two types of CdTe QDs with emissions at 520 and 610 nm were embedded into PNIPAM microgels via hydrogen-bonding interactions. Thermoinduced collapse and swelling of microgels leads to tunable spatial distance between two types of quantum dots; thus, temperature variations can be transformed into ratiometric fluorescence intensity changes.

Innovations in electrochemical sensors with high-throughout methods focusing on detection limit, analysis time and portability provided large-scale consumer markets for inexpensive biosensors for glucose and pregnancy tests using anti-human chorionic gonadotropin immobilization strip with lateral-flow technology. Immobilization of analytes using polymers and nanomaterials are the key to improve the sensitivity and detection limit. In this viewpoint, lateral-flow technology allows direct delivery of samples to desired spot to create specific interactions instead of random. Much of the before mentioned biosensors have used this technology and, in fact, it has paved way for bio-fabrication using either contact or non-contact-based patterning. Use of nanomaterials like gold, silver, and silicon-based bio-fabrication yielded new methods. In addition, coating of polymers on these nanomaterials brought revolution in contact-based electrochemical sensing. One of the major advantages on these types of electrochemical sensors is sensitivity and specificity with real-time analysis. However, the limitations are the regenerative ability or long-term usage of polymers/other materials, yet reduction in cost makes such electrochemical sensors more affordable.

CHAPTER 5

RESULTS AND DISCUSSION

RTDs v/s Thermocouples

Thermocouples are better than RTDs when it comes to cost, ruggedness, measurement speed, and the range of temperatures that can be measured using them. Most thermocouples cost 2.5 to 3 times less than RTDs and although RTD installation is cheaper than thermocouple installation, the savings in installation costs are not enough to tip the balance. Furthermore, thermocouples are designed to be more durable and react faster to changes in temperature because of that same design. However, the main point of thermocouples is their range. Most RTDs are limited to a maximum temperature of 540℃. In contrast, certain thermocouples can be used to measure up to 1400℃

RTDs are superior to thermocouples in that their readings are more accurate and more repeatable. That means users reading the same temperatures produce the same results over multiple trials. RTDs producing more repeatable readings means that their readings are more stable, while their design ensures that RTDs continue producing stable readings longer than thermocouples. Furthermore, RTDs receive more robust signals and it is easier to calibrate RTD readings due to their design.

(Platinum v/s Nickel)

We mostly use platinum wire to build the RTDs Platinum RTDs are best suited for precision applications where absolute accuracy and repeatability is critical. The platinum material is less susceptible to environmental contamination, where copper is prone to corrosion causing long term stability problems. Copper is an exceptional material to use in electronic devices due to its low resistivity and low cost. One drawback that limits the use of copper in electronics is the high temperatures required to attach the copper to the host material. These temperatures range from 200°C to over 400°C. Most processes require 15 minutes to 3 hours in an oven to attach the copper whereas we cure the PDMS on silicon wafer in the range of 70℃ to 75℃. Higher temperatures can shorten the time requirement, but many substrates are not able to withstand the intense heat requirements. Additionally, the high temperatures may allow the copper to diffuse into some substrate materials.

Nickel RTDs tolerate environmental conditions well, however, they are limited to smaller temperature ranges**.** The resistivity of the platinum is higher than the other metals, making the physical size of the element smaller. This offers advantages where "real-estate" is at a premium as well better thermal responsiveness. Nickel and nickel-iron alloys were used because they exhibit higher temperature coefficients and the wire is both much easier to work with and less expensive than platinum. The nickel-iron alloy became popular because the material is made especially for temperature sensor use and its high resistivity supported higher resistance RTDs. While nickel and the nickel alloy are relatively stable. The use of the nickel materials in new sensor designs persists because it may be formed by chemical etching into useful configurations. The bottom line is that platinum is much more stable, and when it comes to long-term measurement of temperature the others are not even close. RTDs are known for their excellent accuracy and linearity over a wide temperature range. This metal is a good compromise between copper and platinum. It has a higher output and is slightly less expensive than platinum. It is extremely nonlinear above 300℃.

Some RTDs have accuracies as high as 0.01 ohms (0.026°C) at 0°C. RTDs are also extremely stable devices. Common industrial RTDs drift less than 0.1°C/year. Manufacturing processes increasingly require precise process control. Because an RTD is a passive resistive device, you must pass a current through the device to produce a measurable voltage. This current causes the RTD to internally heat, which appears as an error. We can minimize self-heating by using the smallest possible excitation current. The typical RTD receiving device uses 1mA to stimulate the RTD.

The roughness factor of the working electrode is very important for electrochemical analysis, since it is proportional to the current response of the electrochemical sensor. The use of nanostructured electrode can improve the performance of electrochemical biosensors due to their high surface area ratio and good electro-catalytic ability for the H2O2. The roughness of the working electrode surface was optimized by multi-cycle cyclic voltammetry (CVs) of the Pt NPs. The inset shows the electrode current outputs versus number of CVs which were measured in 1mM H_2O_2 solution. This measurement was performed at a potential of 600mV versus the potential of the Ag/AgCl (3M NaCl) reference electrode after stabilizing the background current as as nearly constant value. The electrodes with 30 cycles of CVs gave the highest outputs, so it was chosen to construct the lactate biosensors.

5.1 Conductivity Measurements

The coefficient of thermal conductivity, k, is the coefficient of heat transfer (ΔQ) across a steady-state temperature difference (ΔT) during time Δt over a distance (x), in a direction normal to a surface of area A. The working equation is as follows:

$$k = \frac{\Delta Q}{A\Delta t}\frac{x}{\Delta T} \tag{5.1}$$

For thin film Au, the heat transmitted during time Δt:

$$\Delta P = \frac{\Delta Q}{\Delta T} = \int I(R)^2\, dR \tag{5.2}$$

where ΔQ is energy, I is the applied current and R is the resistance. In a special case that I is a constant, define the resistance change over Δt is ΔR, Equation (5.2) can then be expressed as:

$$\Delta P = I^2 * \Delta R \tag{5.3}$$

Thus equation 5.1 can be rewritten as

$$k = \frac{I^2}{A}\Delta R\,\frac{x}{\Delta T} \tag{5.4}$$

the squared current and the measured resistance plotted against the time under different conditions (temperature, thermal conductivity), respectively. The peak currents (I) can be approximated as a constant when it reaches the peak value between 0.3 and 0.4 seconds. The variation in ΔR under different conditions is ±7%. Thus, for simple estimation of the thermal conductivity, the effect of ΔR is neglected. Further simplification is made by if at the peak current, the pseudo steady-state is met, and x/ΔT is the same (ΔT is around 2°C). After these reductions, the thermal conductivity correlates to the peak squared current only.

The relationship between the peak squared currents and the thermal conductivity were measured at the pseudo steady-state at the beginning of the heating period under different conditions. As shown in Figure 5.1, the maximum linearity error is 0.8% even though the simple relationship has been adopted. Based on such relationship, a first order equation can be applied to obtain the thermal conductivity compensated outputs. The method has the advantages of fast estimation of the thermal conductivity (within 100 ms) and implementation of the thermal conductivity compensation without interrupting the sensor operation.

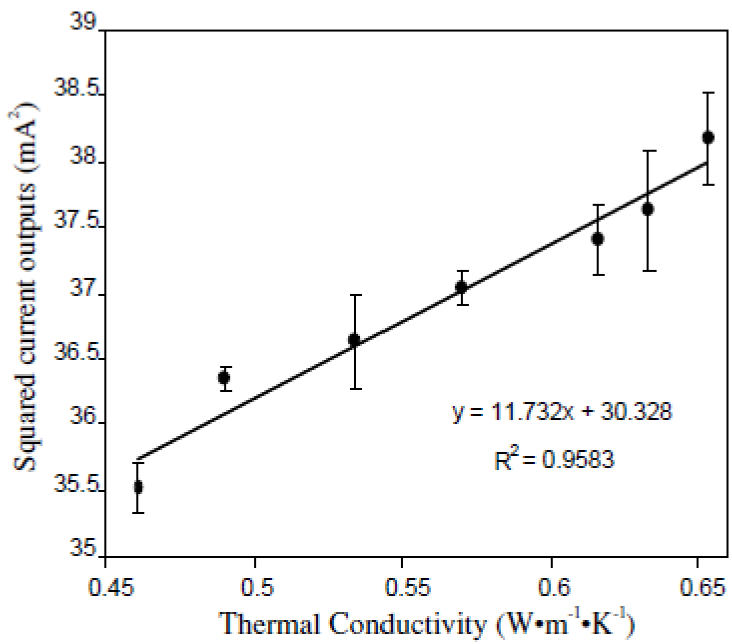

Figure 5.1 Squared peak current of flow sensor in the medium with different thermal conductivity (Glucose solutions: 0.653, 0.633, 0.616, 0.571, 0.534 0.49 and 0.461 W•m-1•K-1). Squared currents were linearly related to the thermal conductivity.
Source Li, C., Wu, P., Hartings, J. A., Wu, Z., Ahn, C. H., & Narayan, R. K. (2012). Cerebral blood flow sensor with in situ temperature and thermal conductivity compensation. 2012 IEEE 25th International Conference on Micro Electro Mechanical Systems (MEMS). doi:10.1109/memsys.2012.6170188.

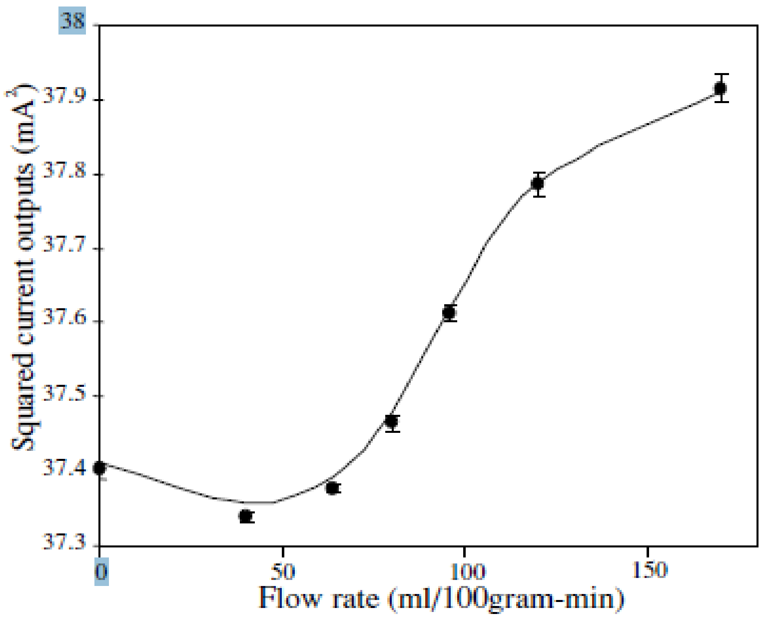

Figure 5.2 The peak squared current versus the flow rate: the current changes under the different flow rates at the same medium. However, the error is within the targeted system resolution with the flow rate below 100ml/100gram-min.

Source Li, C., Wu, P., Hartings, J. A., Wu, Z., Ahn, C. H., & Narayan, R. K. (2012). Cerebral blood flow sensor with in situ temperature and thermal conductivity compensation. 2012 IEEE 25th International Conference on Micro Electro Mechanical Systems (MEMS). doi:10.1109/memsys.2012.6170188.

The effect of different flow rates on the there conductivity measurements has been evaluated. The experimental results in 20°C DI water. The error is around 3.5 ml/100grammin at a flow rate of 96 ml/100gram-min, which is below the targeted system resolution (5 ml/100gram-min). This enables estimation of intrinsic thermal conductivity without no-flow calibration. During operation, three data points associated with the peak outputs were sampled and their average was stored to account for the contribution of medium thermal conductivity to the first order. The compensated flow rate, Fc, is generated from the following linear equation:

$$F_c = \frac{V_u - V_p^2 * G_c - V_0}{S} \tag{5.5}$$

where Vu is the uncompensated output, Vp is the average peak output, Vc is the gain specific for the thermal conductivity compensation, Vo is the baseline voltage, and S the sensor sensitivity. Gc and Vo are derived experimentally under various medium thermal conductivities, and under no flow condition, respectively. The uncompensated and compensated flow sensor outputs versus medium thermal conductivity. The flow sensor was under a constant flow rate of ~50 ml/ 100 g/min. Glucose solutions of different concentrations were used to produce media with different thermal conductivities. The results indicated that using the squared peak currents to compensate the flow sensor outputs can reduce the error from 8.5 ml/100 g/min to 1 ml/100 g/min when the medium undergoes thermal conductivity changes of 0.17 $W \cdot m^{-1} \cdot K^{-1}$.[2]

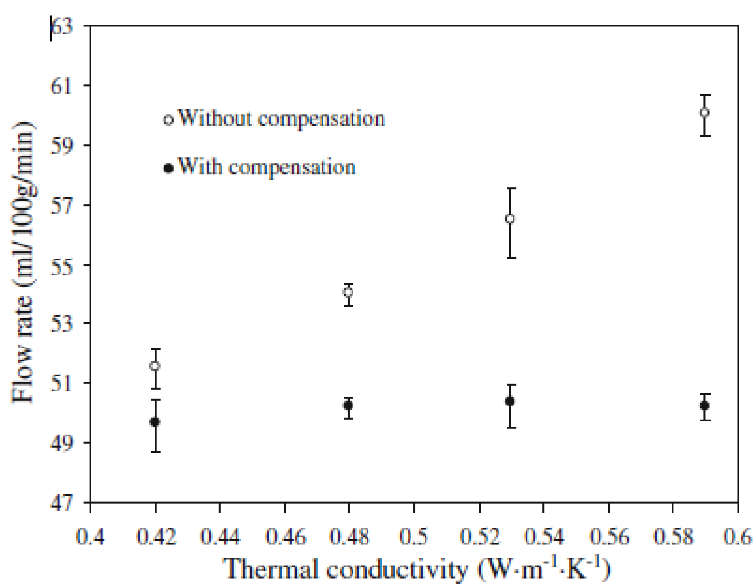

Figure 5.3 Thermal conductivity compensation during the heating period: The flow sensor is subject to the constant flow rate of ~50 ml/100 g/min and the solution with different thermal conductivity was introduced. Using squared peak currents to compensate the flow sensor outputs can reduce the error from 8.5 ml/100 g/min to 1 ml/100 g/min.

Source Li, C., Wu, P., Hartings, J. A., Wu, Z., Cheyuo, C., Wang, P., . . . Narayan, R. K. (2012). Micromachined lab-on-a-tube sensors for simultaneous brain temperature and cerebral blood flow measurements. Biomedical Microdevices,14(4), 759-768. doi:10.1007/s10544-012-9646-7

5.2 Timing Diagram

The LOT temperature sensor operates with AC excitation current of 500 μA. Its output voltage because of the AC excitation shown, where its peak-to-peak value correlates linearly to the temperature. The LOT temperature sensor updates the outputs every 200 milliseconds. When the temperature of the electrically heated LOT flow sensor increases, it loses power to its surrounding until it reaches a thermal equilibrium. An optimal compromise of high temporal resolution and output accuracy is achieved by a cycle of 6s cooling and 4s heating[2]. the sensor output during a complete cooling-heating cycle with the five operation regions.

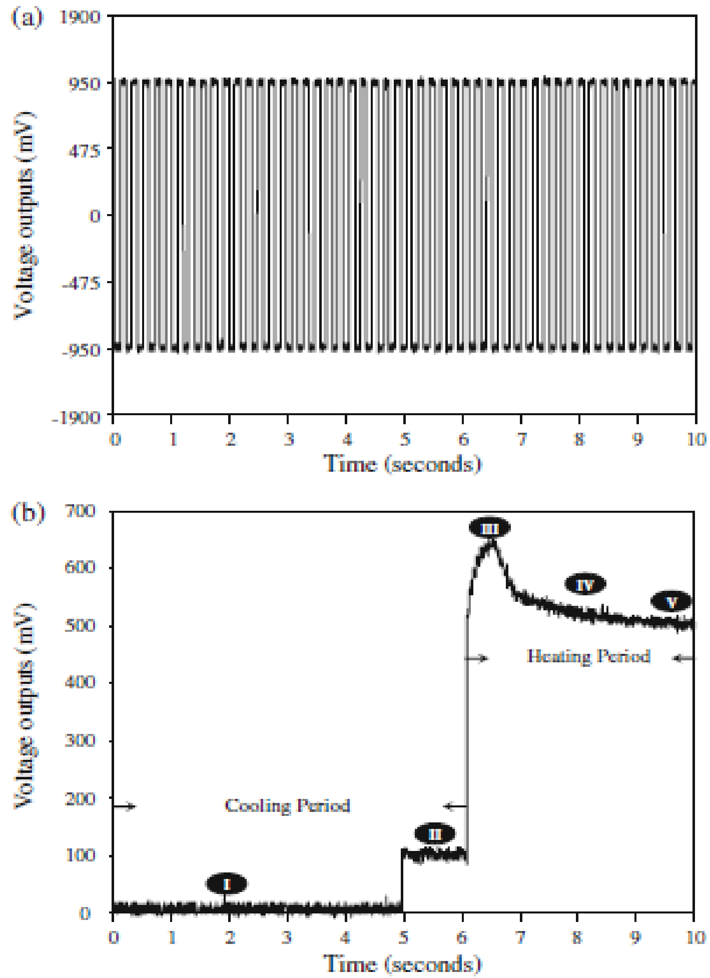

Figure 5.4 Timing diagram: (a) Temperature sensor operates with ac excitation current of 500 μA and 5 Hz. The outputs update every 200 ms. (b) Flow sensor operates with periodic cooling and heating technique. The cooling period (I, II) is 6 s and heating period (III, IV, V) is 4 s. The outputs update every 10s

Source Li, C., Wu, P., Hartings, J. A., Wu, Z., Cheyuo, C., Wang, P., . . . Narayan, R. K. (2012). Micromachined lab-on-a-tube sensors for simultaneous brain temperature and cerebral blood flow measurements. Biomedical Microdevices,14(4), 759-768. doi:10.1007/s10544-012-9646-7

5.3 Sensitivity

Sensitivity of a sensor is defined as the change in output of the sensor per unit change in the parameter being measured. The factor may be constant over the range of the sensor (linear), or it may vary (nonlinear). The temperature sensor in the neural catheter was optimized to measure small transient temperature changes, as those induced by CSD Polyimide (PI2611) film has low thermal conductivity compared to traditional silicon substrate (0.52 vs. 155 W/(K*m)). Thus, thick PI2611 passivation layer may decrease the sensitivity of detecting small transient temperature changes. The sensitivity of two brain temperature sensors with different polyimide layer passivation thicknesses (7 μm and 14 μm thick) was evaluated. The sensor with 14 μm thick passivation was realized by coating the sensor with another 7 μm thick PI2611. The temperature sensors were calibrated using a commercial temperature probe with guaranteed 0.1 °C accuracy. The responses of the two sensors to transient brain temperature changes. CSDs induced by needle prick produced approximately 0.25 °C temperature increases for less than 2 min. Both temperature sensors showed comparable temperature rise, but the temperature increase for the sensor with thick passivation layer was only 65% of that with the thin passivation. The temperature sensor with thin polyimide layer passivation showed higher sensitivity than the other passivation. Thinner passivation layers with improved electrical and moisture resistance for better sensitivity can be achieved with Parylene C or deposition of solid state materials such as Silicon Nitride on the polymer substrates.

5.4 Response Time

The temporal response of a RTD temperature sensor when exposed to instantaneous change in environment temperature is defined by two measures: time constant and response time. Time constant is the time to reach 63.2% of the complete step change in temperature. Response time is the time to reach within 0.5% of the final temperature in a step change. The ability to track process changes depends on the sensor's thermal mass and proximity to the process. The time response for SCTs was determined by moving the SCTs from the ambient air (~25°C) into a water bath at two temperatures, 50°C and 75°C. The two curves are matched well indicating that the time response is independent of the water bath temperature in the SCT operating range. The time constant and response time are found to be around 180 ms and 950 ms, respectively.

5.5 Stability

In practice, the activity of the enzyme decreases with the repeated and continuous use of the biosensors. Enzyme immobilized in a sensing element also slowly leaches out through the outer membrane and gradually loses its activity with time. Therefore, excess enzyme is desired in implantable lactate biosensors to minimize the effect of progressive loss of enzyme activity and to maintain the response sensitivity. We loaded excess enzymes in the 7.5μm deep groove between the working and counter electrodes. The sensitivity over a period of 7 days in the clinical CSF. The calibration of the sensors was carried out five times per day, and average values of sensitivity were displayed. The lactate biosensor retained about 95% of its original response after one week of continuous measurements. The long-term stability is attributed to excess LOD enzyme loading in the groove structure.

CHAPTER 6

CONCLUSION AND RECOMMENDATION FOR FUTURE STUDIES

In this, we have compared the design, operation and performance of a micromachined LOT device with the temperature and flow sensors. Thermal and electronic crosstalk between the sensors was greatly reduced by locating the temperature sensor outside the "thermal influence" region of the flow sensor and by placing the sensors on two different layers with a thin-film Cu shield. Under the working mechanism of AC excitation of the temperature sensor and periodic heating and cooling of the flow sensor, simultaneous temperature and flow rate measurements with a single LOT device were shown to be accurate and reliable in human bloodstained CSF solution over the course of 5 days. Since the LOT microsensors show satisfactory results and have also passed the mechanical, electrical and in vitro cytotoxicity tests which we plan to report in our future publication, they hold promise for *in vivo* evaluation and clinical use. Although LOT device focuses on intracranial monitoring for acute brain injury, we expect that the techniques and prototype developed here can be applied to a variety of tissue monitoring purposes. The polyimide passivation layer thickness and the distance between the temperature and cerebral blood flow sensors were optimized to achieve high sensitivity to transient brain temperature changes and accurate absolute CBF measurements.

The distance between the recording and on-probe reference electrodes for ECoG signals was optimized to achieve high DC stability while not degrading the actual neural signals. The biocompatibility of the neural catheter was examined both by *in vitro* and *in vivo* outcomes. It confirms that the neural catheter is biocompatible in neuronal cell cultures and minimally toxic with long-term *in vivo* implantation. The performance of the neural catheter was assessed in an *in vivo* needle prick model as a translational replica of a traumatic brain injury. Using a single neural catheter, it measures real-time changes in physiological, biochemical and electrophysiological signals. Furthermore, the developed neural catheter can be used for *in situ* drug delivery or CSF sampling for different applications.

The design and evaluation of a micromachined flow sensor with *in situ* temperature and thermal conductivity compensation for continuous measurement of cerebral blood flow have been presented. Thermal conductivity compensation was realized by sampling the peak current outputs at the beginning of the heating period. In spite the simplification and limitations of the measurement methods, the preliminary experimental results validate using the squared peak currents to perform simple thermal conductivity compensation.

The thermal conductivity compensation methods with higher accuracy, such as taking into account the term ΔR, are currently under investigation. The baseline temperature variation during the heating period was also compensated by the integrated temperature sensor. The developed flow sensor and its *in situ* temperature and thermal conductivity compensation methods have numerous applications for biomedical measurements. In this work, the design and evaluation of a lactate biosensor spirally-rolled outside the intraventricular catheter have been presented for early CSF infection detection.

The accuracy of lactate biosensor was greatly improved by doing *in situ* temperature dependency correction and coating the sensors with PVA hydrogels to minimize the oxygen dependency. The groove structure between the working and counter electrodes that can store excess enzymes increased the lactate biosensor’s stability and lifetime. It developed an optimized smart catheter temperature sensor for intracranial temperature monitoring.

Temperature measurements with SCTs have been accurate and reliable in the physiological range of 30- 45°C. The *in vitro* bench test data showed that the standard deviations of all SCTs were small (±0.07°C) and well within the targeted range (±0.1°C). Furthermore, the ability of the SCTs to be integrated with multiple microsensors into a single catheter will make it an attractive choice for multimodality monitoring. After this *in vitro* bench test, the next step will be to conduct a trial of the SCTs in brain tissue in vivo and in comparison with gold-standard clinical methods of measuring intracranial temperature[4].

Despite the rapid progress in biosensor development, clinical applications of biosensors are still rare, with glucose monitor as an exception. This is in sharp contrast to the urgent need in small clinics and point-of-care tests. We believe the following requirements are necessary. First, high sensitivity: Sensitivity improvement is an ever-lasting goal in biosensor development. It is true that the requirement for sensitivity varies from case to case. For example, one does not need a very high sensitivity for glucose detection since glucose concentration is high in blood. This is a part of reason for the success of glucose monitors. However, in many cases it is very important to develop highly sensitive biosensors, optimally single-molecule detection, to meet the requirement of molecular diagnostics and pathogen detection. Second, high selectivity: This might a major barricade in the application of biosensors. Most biosensors reported in the literature work very well in laboratories, however may meet series problems in test real samples. As a result, it is essential to develop novel surface modification approaches to avoid nonspecific adsorption at surfaces. Third, multiplexing is critical for saving assay time, which is especially important for assays performed in laboratories or clinics. It is important to develop miniaturized biosensors to increase portability, thus meet the requirement of field and point-of-care test. Fourth, an ideal biosensor should be integrated and highly automated. Current lab-on-a-chip technologies (microfluidics) offer a solution toward this goal. We can expect that successful biosensors in the future may incorporate all these features, and can conveniently detect minute targets within a short period.

REFERENCES

1. Li, C., Wu, P., Hartings, J. A., Wu, Z., Cheyuo, C., Wang, P., . . . Narayan, R. K. (2012). Micromachined lab-on-a-tube sensors for simultaneous brain temperature and cerebral blood flow measurements. Biomedical Microdevices,14(4), 759-768. doi:10.1007/s10544-012-9646-7

2. Li, C., Wu, Z., Limnuson, K., Cheyuo, C., Wang, P., Ahn, C. H., . . . Hartings, J. A. (2016). Development and application of a microfabricated multimodalneural catheter for neuroscience. Biomedical Microdevices,18(1). doi:10.1007/s10544-016-0034-6

3. Zhang, R. R., Lubin, J. A., & Kuo, J. S. (2016). Bioresorbable Silicon Electronic Sensors for the Brain. Neurosurgery,79(4). doi:10.1227/01.neu.0000499711.96831.af

4. Wu, Z., Li, C., Hartings, J., Narayan, R. K., & Ahn, C. (2016). Polysilicon based flexible temperature sensor for high spatial resolution brain temperature monitoring. 2016 38th Annual International Conference of the IEEE Engineering in Medicine and Biology Society (EMBC). doi:10.1109/embc.2016.7592217

5. Li, C., & Narayan, R. K. (2012). Development of a novel catheter for early diagnosis of bacterial meningitis caused by the ventricular drain. 2012 IEEE 25th International Conference on Micro Electro Mechanical Systems (MEMS). doi:10.1109/memsys.2012.6170108

6. Li, C., Wu, P., Hartings, J. A., Wu, Z., Ahn, C. H., & Narayan, R. K. (2012). Cerebral blood flow sensor with in situ temperature and thermal conductivity compensation. 2012 IEEE 25th International Conference on Micro Electro Mechanical Systems (MEMS). doi:10.1109/memsys.2012.6170188.

7. Zhang, R. R., Lubin, J. A., & Kuo, J. S. (2016). Bioresorbable Silicon Electronic Sensors for the Brain. *Neurosurgery,79*(4). doi:10.1227/01.neu.0000499711.96831.af

8. Boylan, A., Martin, C. J., & Gardner, G. G. (1992). Infrared emissivity of burn wounds. *Clinical Physics and Physiological Measurement,13*(2), 125-127. doi:10.1088/0143-0815/13/2/003.

9. Cenydd, L. A., John, N., Bloj, M., Walter, A., & Phillips, N. (2012). Visualizing the Surface of a Living Human Brain. *IEEE Computer Graphics and Applications,32*(2), 55-65. doi:10.1109/mcg.2011.105.

10. Polysilicon-based flexible temperature sensor for brain monitoring with high spatial resolution. (n.d.). *Polysilicon-based flexible temperature sensor for brain monitoring with high spatial resolution*.

11. Seymour, J. P., Elkasabi, Y. M., Chen, H., Lahann, J., & Kipke, D. R. (2009). The insulation performance of reactive parylene films in implantable electronic devices. *Biomaterials*,*30*(31), 6158-6167. doi:10.1016/j.biomaterials.2009.07.061

12. Liu, P., Zhu, R., & Que, R. (2009). A Flexible Flow Sensor System and Its Characteristics for Fluid Mechanics Measurements. *Sensors*,*9*(12), 9533-9543. doi:10.3390/s91209533

13. Kim, I., Fok, H. H., Li, Y., Jackson, T. N., & Gluckman, B. J. (2011). Polymer substrate temperature sensor array for brain interfaces. *2011 Annual International Conference of the IEEE Engineering in Medicine and Biology Society*. doi:10.1109/iembs.2011.6090892

14. http://www.mfg.mtu.edu/cyberman/machtool/machtool/sensors/fundamental.html

15. http://www.egr.msu.edu/classes/ece445/mason/Files/4-Sensors_ch2.pdf

16. Rosenthal, G., Sanchez-Mejia, R. O., Phan, N., Hemphill, J. C., Martin, C., & Manley, G. T. (2011). Incorporating a parenchymal thermal diffusion cerebral blood flow probe in bedside assessment of cerebral autoregulation and vasoreactivity in patients with severe traumatic brain injury. *Journal of Neurosurgery*,*114*(1), 62-70. doi:10.3171/2010.6.jns091360

17. Zhang, Y., Xiao, X., Zhang, J., Gao, Z., Ji, N., & Zhang, L. (2017). Diagnostic accuracy of routine blood examinations and CSF lactate level for post-neurosurgical bacterial meningitis. *International Journal of Infectious Diseases*. doi:10.1016/j.ijid.2017.03.026

18. Krajewski, K. L., Orakcioglu, B., Haux, D., Hertle, D. N., Santos, E., Kiening, K. L., . . . Sakowitz, O. W. (2011). Cerebral Microdialysis in Acutely Brain-Injured Patients with Spreading Depolarizations. *Early Brain Injury or Cerebral Vasospasm*, 125-130. doi:10.1007/978-3-7091-0353-1_22

19. Li, C., Ahn, C. H., Shutter, L. A., & Narayan, R. K. (2009). Toward real-time continuous brain glucose and oxygen monitoring with a smart catheter. *Biosensors and Bioelectronics*,*25*(1), 173-178. doi:10.1016/j.bios.2009.06.032

20. Kaur, H. (2015). Biosensors: Recent Advancements in Tissue Engineering and Cancer Diagnosis. *Biosensors Journal,04*(02). doi:10.4172/2090-4967.1000131

21. Biosensor, method of producing them and analysis methods using same (A Haouz et al, FR). (1998). *Biofutur,1998*(178), 48. doi:10.1016/s0294-3506(98)80112-9

22. Lai, H., Liao, L., Lin, C., Hsu, J., He, X., Chen, Y., . . . Shih, Y. I. (2012). Design, simulation and experimental validation of a novel flexible neural probe for deep brain stimulation and multichannel recording. *Journal of Neural Engineering,9*(3), 036001. doi:10.1088/1741-2560/9/3/036001

23. Hinzman, J. M., Andaluz, N., Shutter, L. A., Okonkwo, D. O., Pahl, C., Strong, A. J., . . . Hartings, J. A. (2014). Inverse neurovascular coupling to cortical spreading depolarizations in severe brain trauma. *Brain,137*(11), 2960-2972. doi:10.1093/brain/awu241

24. Du, J., Blanche, T. J., Harrison, R. R., Lester, H. A., & Masmanidis, S. C. (2011). Multiplexed, High Density Electrophysiology with Nanofabricated Neural Probes. *PLoS ONE,6*(10). doi:10.1371/journal.pone.0026204